Degeneracy-Preserving Quantum Nondemolition Measurement of Parity-Type Observables for Cat Qubits

Joachim Cohen, W. Clarke Smith, Michel H. Devoret, and Mazyar Mirrahimi

Phys. Rev. Lett. **119**, 060503 — Published 9 August 2017

DOI: 10.1103/PhysRevLett.119.060503

Degeneracy-preserving quantum non-demolition measurement of parity-type observables for cat-qubits

Joachim Cohen[1],* W. Clarke Smith[2],† Michel H. Devoret[2],‡ and Mazyar Mirrahimi[1,3§]
[1] *QUANTIC project-team, INRIA Paris, France*
[2] *Department of Applied Physics, Yale University, New Haven, CT 06520, USA*
[3] *Yale Quantum Institute, Yale University, New Haven, CT 06520, USA*

A central requirement for any quantum error correction scheme is the ability to perform quantum non-demolition measurements of an error syndrome, corresponding to a special symmetry property of the encoding scheme. It is in particular important that such a measurement does not introduce extra error mechanisms, not included in the error model of the correction scheme. In this letter, we ensure such a robustness by designing an interaction with a measurement device that preserves the degeneracy of the measured observable. More precisely, we propose a scheme to perform continuous and quantum non-demolition measurement of photon-number parity in a microwave cavity. This corresponds to the error syndrome in a class of error correcting codes called the cat-codes, which have recently proven to be efficient and versatile for quantum information processing. In our design, we exploit the strongly nonlinear Hamiltonian of a high-impedance Josephson circuit, coupling a high-Q cavity storage cavity mode to a low-Q readout one. By driving the readout resonator at its resonance, the phase of the reflected/transmitted signal carries directly exploitable information on parity-type observables for encoded cat-qubits of the high-Q mode.

By encoding a qubit in a superposition of coherent states of a harmonic oscillator, one benefits from the redundancy provided by the infinite dimensional Hilbert space of the system to realize a quantum error correction (QEC) protocol. In a set of theoretical and experimental results, various aspects of encoding [1, 2], manipulation [3–6], error syndrome measurement [7] and full quantum error correction [8, 9] with these states have been explored. Most spectacularly, a recent experiment [9] demonstrated an enhancement of the error-corrected cat-code's lifetime with respect to all system components. The performance of the error correction is however limited by uncorrected error channels such as deterministic relaxation of the coherent states amplitude, dephasing induced by cavity's inherited anharmonicity, and most significantly the propagating errors from the ancillary transmon [10] used for error syndrome measurements.

In an effort towards a fault-tolerant and scalable architecture for quantum information processing, we recently proposed a framework based on non-linear drives and dissipations to dynamically protect a degenerate manifold spanned by two or four coherent states against some of these error channels [3]. Indeed, by engineering a non-linear coupling to a driven bath where the exchange of photons occurs mainly in pairs (or quadruples) of photons, one can stabilize a manifold spanned by two (resp. four) coherent states $\mathcal{M}_{2,\alpha} = \text{span}\{|\pm\alpha\rangle\}$ (resp. $\mathcal{M}_{4,\alpha} = \text{span}\{|\pm\alpha\rangle, |\pm i\alpha\rangle\}$). This stabilization suppresses, exponentially in $|\alpha|^2$, the phase-flip errors of a logical qubit given by $|0\rangle_L = |\mathcal{C}_\alpha^+\rangle, |1\rangle_L = |\mathcal{C}_\alpha^-\rangle$ (resp. $|0\rangle_L = |\mathcal{C}_\alpha^{(0\text{mod}4)}\rangle, |1\rangle_L = |\mathcal{C}_\alpha^{(2\text{mod}4)}\rangle$) where, $|\mathcal{C}_\alpha^\pm\rangle = \mathcal{N}_\pm(|\alpha\rangle \pm |-\alpha\rangle)$, $|\mathcal{C}_\alpha^{(0\text{mod}4)}\rangle = \mathcal{N}_0(|\mathcal{C}_\alpha^+\rangle + |\mathcal{C}_{i\alpha}^+\rangle), |\mathcal{C}_\alpha^{(2\text{mod}4)}\rangle = \mathcal{N}_2(|\mathcal{C}_\alpha^+\rangle - |\mathcal{C}_{i\alpha}^+\rangle), |\mathcal{C}_\alpha^{(1\text{mod}4)}\rangle = \mathcal{N}_1(|\mathcal{C}_\alpha^-\rangle - i|\mathcal{C}_{i\alpha}^-\rangle), |\mathcal{C}_\alpha^{(3\text{mod}4)}\rangle = \mathcal{N}_3(|\mathcal{C}_\alpha^-\rangle + i|\mathcal{C}_{i\alpha}^-\rangle)$, and $\mathcal{N}_\pm, \mathcal{N}_{0,1,2,3}$ are normalization constants near $1/\sqrt{2}$. One therefore deals with logical qubits that are only susceptible to bit-flip errors. These errors can next be suppressed to first order by photon-number parity measurements as in [9]. Also, one can achieve higher-order correction through a register of such logical qubits and performing joint parity measurements between adjacent ones.

While initial experiments with two-photon driven dissipation [11] illustrate the viability of such a framework, many theoretical and experimental improvements are required in order to achieve a fully fault-tolerant architecture. One very important improvement concerns the quantum non-demolition (QND) measurement protocols for parity-type observables. Such single-mode or two-mode photon number parity measurements have been performed using an ancillary transmon and a Ramsey interferometry type scheme [6, 7, 12]. These measurements however are not fault-tolerant and represent the main limitation in QEC [9]. In this letter, we propose a new framework to perform QND measurement of various parity-type observables which could be integrated in a fault-tolerant architecture.

The current measurement schemes [6, 7] are based on a dispersive coupling of the cavity mode to a transmon through a Hamiltonian of the form $-\hbar\chi|e\rangle\langle e|\mathbf{a}^\dagger\mathbf{a}$. The parity measurement is performed by initializing the

*Electronic address: joachim.cohen@inria.fr
†Electronic address: clarke.smith@yale.edu
‡Electronic address: michel.devoret@yale.edu
§Electronic address: mazyar.mirrahimi@inria.fr

transmon in the superposition $(|g\rangle+|e\rangle)/\sqrt{2}$ and waiting for a time π/χ. The $|e\rangle$ state of transmon acquires a π phase only for odd cavity Fock states. A measurement of the transmon, distinguishing between $(|g\rangle+|e\rangle)/\sqrt{2}$ and $(|g\rangle-|e\rangle)/\sqrt{2}$ indicates the photon number parity. Nevertheless, a T_1 error of the transmon during the evolution propagates to the cavity mode inducing photon dephasing. Indeed, such a measurement protocol is not fault-tolerant as the eigenstates of the measured observable (here parity cat states) get entangled to the ancillary system during the measurement protocol, making them vulnerable to the ancilla's errors (here T_1 errors): a cat state $|\mathcal{C}_\alpha^\pm\rangle$ evolves to $(|\mathcal{C}_\alpha^\pm\rangle\otimes|g\rangle+|\mathcal{C}_{\alpha e^{-i\chi t}}^\pm\rangle\otimes|e\rangle)/\sqrt{2}$. A fault-tolerant parity measurement could be for instance achieved through an effective Hamiltonian of the form $\hbar\chi|e\rangle\langle e|\cos(\pi\mathbf{a}^\dagger\mathbf{a})$. A cat state $|\mathcal{C}_\alpha^\pm\rangle$ would then evolve to $|\mathcal{C}_\alpha^\pm\rangle\otimes(|g\rangle+e^{\pm i\chi t}|e\rangle)/\sqrt{2}$, without entangling to the transmon.

While the engineering of a highly degenerate Hamiltonian of the form $\hbar\chi\cos(\pi\mathbf{a}^\dagger\mathbf{a})$ seems to be a complicated task, we show that in presence of two-photon or four-photon driven dissipation, it could be effectively achieved with the help of quantum Zeno dynamics [13]. By confining the dynamics to the manifold $\mathcal{M}_{2,\alpha}$, a physical Hamiltonian $\mathbf{H}$ acts as a projected one $\mathbf{H}_{\mathcal{M}_{2,\alpha}}=\Pi_{\mathcal{M}_{2,\alpha}}\mathbf{H}\Pi_{\mathcal{M}_{2,\alpha}}$, where $\Pi_{\mathcal{M}_{2,\alpha}}$ represents the projector on $\mathcal{M}_{2,\alpha}$. To achieve an effective parity Hamiltonian, one requires a physical Hamiltonian $\mathbf{H}$, such that its projection on $\mathcal{M}_{2,\alpha}$ is equivalent to the projection of $\hbar\chi\cos(\pi\mathbf{a}^\dagger\mathbf{a})$ on the same manifold. This means $\mathbf{H}_{\mathcal{M}_{2,\alpha}}=\hbar\chi\Pi_{\mathcal{M}_{2,\alpha}}\cos(\pi\mathbf{a}^\dagger\mathbf{a})\Pi_{\mathcal{M}_{2,\alpha}}=\hbar\chi\boldsymbol{\sigma}_z^L$, where $\boldsymbol{\sigma}_z^L$ is the Pauli operator along the z-axis of the logical qubit defined by $\{|\mathcal{C}_\alpha^\pm\rangle\}$ and well-approximated by $|\alpha\rangle\langle-\alpha|+|-\alpha\rangle\langle\alpha|$. Therefore, $\mathbf{H}$ should couple the two coherent states $|\pm\alpha\rangle$. In the context of quantum superconducting circuits, such a Hamiltonian can be achieved by strongly coupling a high impedance cavity mode to a Josephson junction [14–16]. Indeed, considering a cavity mode with frequency ω_a coupled capacitively to a Josephson junction, and assuming that other modes (including the junction mode) are never excited, the effective Hamiltonian in the interaction picture will be of the form

$$\mathbf{H}_{\rm int}(t)=-\frac{E_J}{2}(\mathbf{D}[\beta(t)]+\mathbf{D}^\dagger[\beta(t)]),\quad \beta(t)=i\varphi_a e^{i\omega_a t}.$$

Here E_J is the effective Josephson energy and $\varphi_a=\sqrt{Z_a/2R_Q}$, where Z_a is the impedance of the cavity mode seen by the junction and $R_Q=(2e)^2/\hbar$ is the superconducting resistance quantum. Moreover, $\mathbf{D}[\beta(t)]$ is the displacement operator defined by $\mathbf{D}[\beta(t)]=e^{\beta(t)\mathbf{a}^\dagger-\beta(t)^*\mathbf{a}}$. For $\varphi_a\approx 2|\alpha|$, this Hamiltonian couples the two coherent states $|\pm\alpha\rangle$. While a practical realization of such a high impedance cavity mode is discussed later, we provide here a precise analysis of the effective Hamiltonian.

In the limit $\hbar\omega_a\gg E_J$, we can apply a rotating wave approximation (RWA) to $\mathbf{H}_{\rm int}(t)$ [17–19], leading to

$$\mathbf{H}^{\rm RWA}=-E_J e^{-\frac{\varphi_a^2}{2}}\sum_n L_n(\varphi_a^2)|n\rangle\langle n|, \qquad (1)$$

where $L_n(.)$ is the Laguerre polynomial of order n. In the presence of two-photon loss, and under the condition $\varphi_a\approx 2|\alpha|$, the effective Hamiltonian takes the form of the parity Hamiltonian, i.e

$$\mathbf{H}^{\rm RWA}_{\mathcal{M}_{2,\alpha}}=-\frac{\hbar\Omega_a}{2}\boldsymbol{\sigma}_z^L+\mathcal{O}(E_J e^{-\frac{\varphi_a^2}{2}}), \qquad (2)$$

where $\boldsymbol{\sigma}_z^L=|\mathcal{C}_\alpha^+\rangle\langle\mathcal{C}_\alpha^+|-|\mathcal{C}_\alpha^-\rangle\langle\mathcal{C}_\alpha^-|$, and Ω_a is a function of E_J, φ_a and α. It is well approximated by $\Omega_a=E_J e^{-\frac{1}{2}(\varphi_a-2|\alpha|)^2}/\hbar\sqrt{\pi|\alpha|\varphi_a}$ [20]. This result is illustrated in Fig. 1(a) and Fig. 1(b).

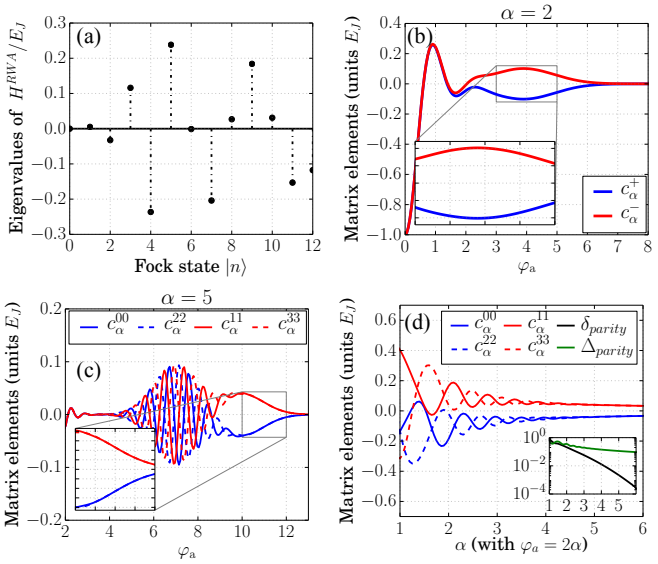

FIG. 1: (a) Eigenvalues of $\mathbf{H}^{\rm RWA}/E_J$ for $\varphi_a=4$. The changing signs around the Fock state $|4\rangle$ explain why under two or four-photon process, the Hamiltonian acts as a parity Hamiltonian for a coherence state $|\alpha\rangle$ with $|\alpha|=\varphi_a/2=2$. Although the parity operator $\cos(\pi\mathbf{a}^\dagger\mathbf{a})$ requires also its eigenvalues to have the same module, this sign alternance is sufficient for having a parity Hamiltonian under two-photon loss. (b) Non-vanishing matrix elements of projected Hamiltonian for the two-photon driven dissipation, $c_\alpha^\pm=\langle\mathcal{C}_\alpha^\pm|\mathbf{H}^{\rm RWA}|\mathcal{C}_\alpha^\pm\rangle$ as a function of φ_a (α being set to 2). As shown in the inset, $c_\alpha^\pm$ take opposite values for $3<\varphi_a<5$, indicating that the projected Hamiltonian acts as the $\boldsymbol{\sigma}_Z$ Pauli operator in the logical basis $|\mathcal{C}_\alpha^\pm\rangle$. (c) Non-vanishing matrix elements of projected Hamiltonian for the four-photon driven dissipation, $c_\alpha^{jj}=\langle\mathcal{C}_\alpha^{(j\,\mathrm{mod}\,4)}|\mathbf{H}^{\rm RWA}|\mathcal{C}_\alpha^{(j\,\mathrm{mod}\,4)}\rangle$ as a function of φ_a (α being set to 5). We note that for $9<\varphi_a<12$, the Hamiltonian is degenerate in each parity subspace. (d) Effect of the amplitude $|\alpha|$ on the parity-subspace degeneracy for the 4-photon process. Fixing $\varphi_a=2\alpha$, we observe that for $\alpha<4$, we deal with a non-degenerate Hamiltonian (hence the choice of $\alpha=5$ in (c)). The inset illustrates that while the parity Hamiltonian strength $\Delta_{\rm parity}=\sqrt{(c_\alpha^{00}-c_\alpha^{11})^2+(c_\alpha^{22}-c_\alpha^{33})^2}$ decreases in $1/|\alpha|$, the parity subspace non-degeneracy $\delta_{\rm parity}=\sqrt{(c_\alpha^{00}-c_\alpha^{22})^2+(c_\alpha^{11}-c_\alpha^{33})^2}$ decreases exponentially in $|\alpha|^2$.

From the construction of a single-mode parity Hamiltonian, acting as a $\boldsymbol{\sigma}_z^L$ Pauli operator in the logical basis, stems an immediate route to build a joint-parity Hamiltonian of two cavity modes **a** and **b** both subject to two-photon dissipation. Considering two cavity modes **a** and **b** coupled to a Josephson junction, the interaction Hamiltonian reads $\mathbf{H}_{int}(t) = -E_J \cos[\varphi_a(\mathbf{a}e^{-i\omega_a t}+c.c)+\varphi_b(\mathbf{b}e^{-i\omega_b t}+c.c)]$. The mode frequencies ω_a and ω_b are off-resonant so that we can apply the RWA (one needs to also avoid high-order resonances)

$$\mathbf{H}^{\rm RWA} = -E_J e^{-\frac{\varphi_a^2+\varphi_b^2}{2}} \sum_{n_a,n_b} L_{n_a}(\varphi_a^2)L_{n_b}(\varphi_b^2)|n_a,n_b\rangle\langle n_a,n_b|.$$

If both **a** and **b** are high-impedance modes and are subject to two-photon loss, one can choose $|\alpha| \approx \varphi_a/2$ and $|\beta| \approx \varphi_b/2$, such that the confined Hamiltonian takes the form $\mathbf{H}^{\rm RWA}_{\mathcal{M}_{2,\alpha,\beta}} = -\frac{\hbar\Omega_{a,b}}{2}\boldsymbol{\sigma}_Z^{a,L}\otimes\boldsymbol{\sigma}_Z^{b,L}$, where $\Omega_{a,b} = \hbar\Omega_a\Omega_b/2E_J$, $\boldsymbol{\sigma}_Z^{a(b),L} = |\mathcal{C}^+_{\alpha(\beta)}\rangle\langle\mathcal{C}^+_{\alpha(\beta)}| - |\mathcal{C}^-_{\alpha(\beta)}\rangle\langle\mathcal{C}^-_{\alpha(\beta)}|$.

We have seen that under two-photon loss, $\mathbf{H}^{\rm RWA}$ acts as a parity Hamiltonian. Remarkably, this result also holds in the presence of four-photon loss, where the dynamics is confined to the larger manifold $\mathcal{M}_{4,\alpha} = \mathcal{M}_{2,\alpha}\oplus\mathcal{M}_{2,i\alpha}$ (Fig. 1(c)). More precisely, for $\varphi_a \approx 2|\alpha|$, the projection of $\mathbf{H}^{\rm RWA}$ on $\mathcal{M}_{4,\alpha}$ satisfies $\mathbf{H}^{\rm RWA}_{\mathcal{M}_{4,\alpha}} = -\hbar\Omega_a/2\,(\boldsymbol{\pi}_{\rm 4ph} + O(e^{-\xi|\alpha|^2}))$, with $\boldsymbol{\pi}_{\rm 4ph} = |\mathcal{C}_\alpha^{(0{\rm mod}4)}\rangle\langle\mathcal{C}_\alpha^{(0{\rm mod}4)}| + |\mathcal{C}_\alpha^{(2{\rm mod}4)}\rangle\langle\mathcal{C}_\alpha^{(2{\rm mod}4)}| - |\mathcal{C}_\alpha^{(1{\rm mod}4)}\rangle\langle\mathcal{C}_\alpha^{(1{\rm mod}4)}| - |\mathcal{C}_\alpha^{(3{\rm mod}4)}\rangle\langle\mathcal{C}_\alpha^{(3{\rm mod}4)}|$ and $\xi = (\sqrt{2}-1)^2 \approx 0.17$ [20]. The undesired term that scales as $e^{-\xi|\alpha|^2}$ lifts the degeneracy within the parity subspaces. This non-degeneracy is however suppressed exponentially with cat size $|\alpha|^2$, while the effective Hamiltonian strength decreases only linearly in $|\alpha|^{-1}$ (Fig. 1(d)). Therefore for large enough α's we still achieve an effective parity Hamiltonian. The perfect degeneracy, for cat states of smaller amplitude, can also be achieved by introducing more junctions providing more degrees of freedom [20].

Following the same idea as in the usual dispersive measurements of superconducting qubits [22], one can perform a continuous QND measurement of the above observables, $\boldsymbol{\sigma}_Z^L$ and $\boldsymbol{\sigma}_Z^L\otimes\boldsymbol{\sigma}_Z^L$ for the two-photon dissipation scheme, and $\boldsymbol{\pi}_{\rm 4ph}$ for the four-photon dissipation. This can be done by coupling an extra off-resonant readout mode to the same junction. This mode is then driven at its resonance (Fig. 2) and the measurement outcome is imprinted on the phase of the reflected signal. More precisely, by coupling a driven readout mode **c** to the junction, and in the case of $\varphi_c\sqrt{n_c} \ll 1$ (here n_c denotes the average number of readout photons and this requirement is equivalent to assuming $n_c \ll n_{\rm crit}$, the critical number for dispersive approximation [23]), we achieve

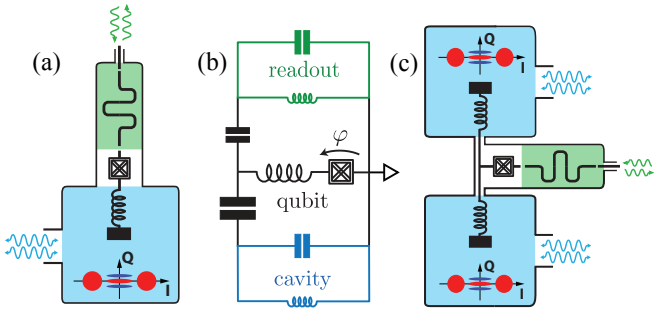

FIG. 2: (a) Schematic of a realization of a single-mode continuous parity measurement in presence of two-photon driven dissipation. Similarly to [21], on one side we mediate a two-photon dissipation of the storage high-Q cavity mode and on the other, we couple to a low-Q readout mode through a high-impedance Josephson circuit. (b) Electrical circuit equivalent, without the two-photon driven dissipation. The cavity (blue) and readout (green) modes are modeled by LC oscillators, and are capacitively coupled to a high impedance Josephson circuit mode. This Josephson mode consists of a large superinductance, formed from an array of large Josephson junctions (as in the fluxonium [14]), in series with a nonlinear circuit element, depicted as a cross-hatched box. (c) Schematic design of the joint-parity measurements between two high-Q cavity modes under two-photon driven dissipation, inspired from [6] and based on an extension of (a).

the effective Hamiltonians:

$$\begin{aligned}
\mathbf{H}^{\rm disp}_{\mathcal{M}_{2,\alpha}} &\approx -\frac{\hbar\widetilde{\Omega}_a}{2}\boldsymbol{\sigma}_Z^a + \frac{\hbar\chi_a}{2}\boldsymbol{\sigma}_Z^a\mathbf{c}^\dagger\mathbf{c} + \mathbf{H}_{\rm drive}(t),\\
\mathbf{H}^{\rm disp}_{\mathcal{M}_{2,\alpha,\beta}} &\approx -\frac{\hbar\widetilde{\Omega}_{a,b}}{2}\boldsymbol{\sigma}_Z^a\boldsymbol{\sigma}_Z^b + \frac{\hbar\chi_{a,b}}{2}\boldsymbol{\sigma}_Z^a\boldsymbol{\sigma}_Z^b\mathbf{c}^\dagger\mathbf{c} + \mathbf{H}_{\rm drive}(t),\\
\mathbf{H}^{\rm disp}_{\mathcal{M}_{4,\alpha}} &\approx -\frac{\hbar\widetilde{\Omega}_a}{2}\boldsymbol{\pi}_{\rm 4ph} + \frac{\hbar\chi_a}{2}\boldsymbol{\pi}_{\rm 4ph}\mathbf{c}^\dagger\mathbf{c} + \mathbf{H}_{\rm drive}(t). \qquad (3)
\end{aligned}$$

Here $\mathbf{H}_{\rm drive}(t) = \hbar(\epsilon_c(t)\mathbf{c}^\dagger + \epsilon_c^*(t)\mathbf{c})$, $\widetilde{\Omega}_a = e^{-\varphi_c^2/2}\Omega_a$, $\widetilde{\Omega}_{a,b} = e^{-\varphi_c^2/2}\Omega_{a,b}$, $\chi_a = \widetilde{\Omega}_a\varphi_c^2$, $\chi_{a,b} = \widetilde{\Omega}_{a,b}\varphi_c^2$.

The first terms in the above Hamiltonians simply induce deterministic rotations in the associated parity subspaces, whereas the second terms correspond to frequency pulls on mode **c** that depend on the values of associated observables. By driving the mode **c** at resonance, the measurement outcome is imprinted on the phase of the pointer coherent state. Taking κ_c to be the dissipation rate of **c** induced by its coupling to a transmission line, the measurement rate is optimal when $\kappa_c = \chi_a$ ($\chi_{a,b}$ for joint-parity measurement) [24]. This optimal rate is given by (see Fig. 3)

$$\Gamma_m^a = \bar{n}_c\chi_a = \bar{n}_c\varphi_c^2 e^{-\frac{\varphi_c^2}{2}}\frac{E_J}{\hbar}\frac{e^{-\frac{1}{2}(\varphi_a-2|\alpha|)^2}}{\sqrt{\pi|\alpha|\varphi_a}}, \qquad (4)$$

$$\Gamma_m^{a,b} = \bar{n}_c\chi_{a,b} = \bar{n}_c\varphi_c^2 e^{-\frac{\varphi_c^2}{2}}\frac{E_J}{\hbar}\frac{e^{-\frac{1}{2}(\varphi_a-2|\alpha|)^2-\frac{1}{2}(\varphi_b-2|\beta|)^2}}{2\pi\sqrt{|\alpha\beta|\varphi_a\varphi_b}}.$$

Practical realization of a high impedance cavity mode, satisfying $\varphi_a \approx 2|\alpha|$, poses a notable challenge. To

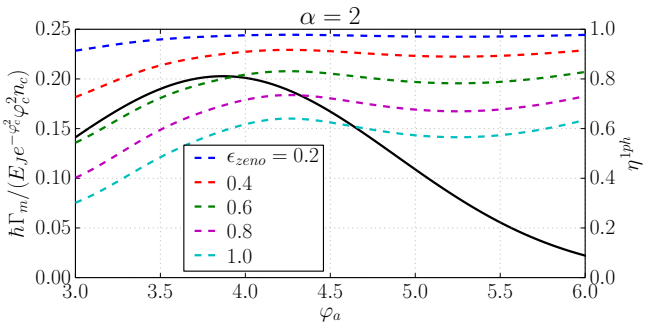

FIG. 3: The left axis (black straight curve) illustrates the measurement rate in the single-mode case (4) in units of $E_J/\hbar$ and renormalized by the parameters of the readout mode. We observe an optimal measurement rate around $\varphi_a = 2\alpha$. The right axis (colored dashed curves) illustrate the efficiency of the measurement limited by the higher order Zeno effects (simulating (5)). Here, we fix $\varphi_c = .1$ and the number of readout photons $n_c = 1$, and we plot $\eta_{1\text{ph}} = \Gamma_m^{1\text{ph}}/(\Gamma_m^{1\text{ph}} + \Gamma_Z)$. This efficiency achieves a local optimum near $\varphi_a = 2\alpha$ corresponding also to the optimum measurement rate Γ_m. This higher-order effect is suppressed by decreasing the Zeno parameter $\epsilon_{\text{zeno}} = E_J/\hbar\kappa_{2ph}$.

see this, note that this relation for $\alpha = 2$ requires an impedance $Z_a = 32R_Q$. For comparison, typical superconducting cavities have impedances $0.1R_Q < Z_a < R_Q$ [25, 26]. However, much larger impedances $Z \sim 8R_Q$ have been produced using devices comprising superinductances (fabricated from arrays of large Josephson junctions), such as in the fluxonium qubit [14–16].

In our proposed experimental system (see Figs. 2a-b), a fluxonium-based qubit mode composed of a superinductance in series with a nonlinear circuit element is capacitively coupled to two cavities. This nonlinear circuit element is assumed to have a Josephson junction-like Hamiltonian of the form $\mathbf{H}_{\text{el}} = 4E_C\mathbf{n}^2 - E_J\cos\mu\boldsymbol{\varphi}$, where $\mathbf{n}$ is the number of Cooper pairs across the element, $\boldsymbol{\varphi}$ is the superconducting phase, E_C is the charging energy, E_J is the Josephson energy, and μ is an integer-valued parameter determined by the implementation. It may be worthwhile to realize $\mu > 1$, and this could be achieved by circuits similar to those proposed in [27, 28]. This transforms the effective cavity impedance according to $Z_a \to \mu^2 Z_a$, making the relation $\varphi_a \approx 2|\alpha|$ much easier to satisfy. The details of this strategy will be described in a forthcoming publication.

Let us now study the limitations of such a measurement protocol. We have made a few approximations and the main limitations are due to second order effects. The first one concerns the RWA. Indeed, dealing with high-impedance modes one needs to be cautious about higher order resonances. While in the single-mode case, such second-order effects lead to a slight modification of the measurement rate, in the two-mode case, they could lead to a small dephasing within the parity subspaces [20]. These effects could be minimized by a careful choice of resonance frequencies.

Another limitation concerns the Zeno approximation. The projected Hamiltonian $\mathbf{H}^{\text{RWA}}_{\mathcal{M}_{2,\alpha}}$ corresponds to a first order Zeno dynamics approximation in $\epsilon_{\text{zeno}} = E_J/\hbar\kappa_{2ph}$ [29, 30]. The second order correction in ϵ_{zeno} induces a dephasing in the basis $\{|\mathcal{C}_\alpha^\pm\rangle\}$ occurring at a rate $\Gamma_Z = r(\alpha,\varphi_a)\epsilon_{\text{zeno}}^2\kappa_{2ph}$, where the numerical factor $r(\alpha,\varphi_a)$ can be derived from [30]. This could be seen as an inefficiency in the measurement, where a constant part (independent of the number of readout photons) of the measurement signal is lost through the two-photon decay channel. Here, we analyze numerically this second order effect by simulating the master equation

$$\frac{d\boldsymbol{\rho}}{dt} = -\frac{i}{\hbar}[\mathbf{H}^{\text{RWA}}, \boldsymbol{\rho}] + \kappa_{2ph}\mathbf{D}[\mathbf{a}^2 - \alpha^2](\rho) \qquad (5)$$

where the single mode Hamiltonian, $\mathbf{H}^{\text{RWA}}$, is given by (1) and $\boldsymbol{\rho}(0) = \frac{1}{2}(|\mathcal{C}_\alpha^+\rangle + |\mathcal{C}_\alpha^-\rangle)(\langle\mathcal{C}_\alpha^+| + \langle\mathcal{C}_\alpha^-|)$. Taking $\alpha = 2$, and varying φ_a and the Zeno parameter ϵ_{zeno}, we look at the decay of purity with time. This corresponds to a dephasing due to higher order Zeno dynamics well-approximated by Γ_Z. We illustrate in Fig. 3 (dashed lines, right axis) the value of $\eta_{1\text{ph}} = \Gamma_m^{1\text{ph}}/(\Gamma_m^{1\text{ph}} + \Gamma_Z)$ corresponding to the measurement efficiency with number of readout photons fixed to $n_c = 1$. As Γ_Z does not depend on the number of readout photons while Γ_m increases linearly in n_c, this efficiency improves for higher number of readout photons. We observe that for a given Zeno parameter ϵ_{zeno}, the point $\varphi_a \approx 2\alpha$ corresponding to the optimal measurement rate Γ_m, is also a local optimum of the efficiency. We do not account for the readout mode $\mathbf{c}$ in these simulations, as it does not contribute to higher-order Zeno approximations and therefore to Γ_Z. This measurement inefficiency is the only detrimental effect of such higher-order dynamics. As the Hamiltonian $\mathbf{H}^{\text{RWA}}$ is diagonal in the Fock states basis, it does not change the parity and therefore do not lead to any bit-flip type error of the logical qubit. The coupling, through the novel Josephson circuit, between the storage cavity to modes that would be anomalously excited, will generate another source of inefficiency. Note that such couplings, in presence of nonlinear dissipation, have no effect more serious than simply unread parity measurements, and do not lead to uncorrectable errors.

We can perform a similar analysis for the two-mode joint-parity measurement protocol. While higher order Zeno dynamics cannot lead to any change of photon number parities (Hamiltonian is diagonal in the Fock states basis), in principle, it can lead to a dephasing for each logical qubit. However, to a very good approximation (exponentially precise in $|\alpha|^2$), such a dephasing occurs in a correlated manner, giving rise to a dissipation channel of the form $\boldsymbol{\sigma}_Z^a \otimes \boldsymbol{\sigma}_Z^b$ [20]. Therefore such higher order effects do not induce any decoherence within a given joint-parity subspace. We thus deal with a QND measurement (with non-unit efficiency) of joint parity.

We have shown how to achieve continuous QND measurement of three parity-type observables for harmonic oscillators. We focus on the case of multi-photon driven

dissipative systems previously introduced for universal quantum computation with cat-qubits [3]. The three observables consist of $\boldsymbol{\sigma}_Z^a = |\mathcal{C}_\alpha^+\rangle\langle\mathcal{C}_\alpha^+| - |\mathcal{C}_\alpha^-\rangle\langle\mathcal{C}_\alpha^-|$ for a single-mode under two-photon process, joint-parity $\boldsymbol{\sigma}_Z^a \otimes \boldsymbol{\sigma}_Z^b$ for two modes under two-photon process, and $\boldsymbol{\pi}_{4\text{ph}} = |\mathcal{C}_\alpha^{(0\text{mod}4)}\rangle\langle\mathcal{C}_\alpha^{(0\text{mod}4)}| + |\mathcal{C}_\alpha^{(2\text{mod}4)}\rangle\langle\mathcal{C}_\alpha^{(2\text{mod}4)}| - |\mathcal{C}_\alpha^{(1\text{mod}4)}\rangle\langle\mathcal{C}_\alpha^{(1\text{mod}4)}| - |\mathcal{C}_\alpha^{(3\text{mod}4)}\rangle\langle\mathcal{C}_\alpha^{(3\text{mod}4)}|$ under four-photon process. We also propose a possible implementation of these measurements through the high-impedance coupling of the cavity mode(s) to a Josephson junction. The fault-tolerant aspect of this measurement protocol plays a crucial rule in the lifetime improvement through a QEC protocol. Indeed, using experimental parameters that are within the reach of current experiments, we predict that this fault-tolerance leads to a lifetime improvement of at least 2 orders of magnitude higher than protocols based on non-fault-tolerant parity measurement [20].

This scheme could also be adapted to non-dissipative cases such as [31]. In presence of strong Kerr type non-linearities, the Hamiltonian perturbation due to high-impedance coupling to a Josephson circuit results in the creation of a parity Hamiltonian. More precisely, considering a cavity subjected to strong self-Kerr effect and a two-photon drive, the Hamiltonian, in the interaction picture, is given by $\mathbf{H}_0 = -\hbar K(\mathbf{a}^{\dagger 2} - \frac{\mathcal{E}_p^*}{K})(\mathbf{a}^2 - \frac{\mathcal{E}_p}{K})$, with K the self-Kerr coefficient, and $\mathcal{E}_p$ the two-photon drive strength [31]. The 2D-manifold $\mathcal{M}_{2,\alpha} = \text{span}\{|\mathcal{C}_\alpha^\pm\rangle\}$ is a doubly degenerate eigenspace of $\mathbf{H}_0$, separated from the other eigenspaces by an energy gap of order $4\hbar|\mathcal{E}_p|$. Considering the first order effect of a perturbative Hamiltonian $\mathbf{H}_1 = \mathbf{H}^{\text{RWA}}$ (see expression (1)) with $||\mathbf{H}_1|| \ll 4\hbar|\mathcal{E}_p|$, we lift the degeneracy of $\mathcal{M}_{2,\alpha}$, leading to two non-degenerate eigenstates approximately given by $|\mathcal{C}_\alpha^+\rangle$ and $|\mathcal{C}_\alpha^-\rangle$. This implies that we have achieved an effective $\boldsymbol{\sigma}_z$ Hamiltonian on the logical basis of cat states.

This research was supported by Inria's DPEI under the TAQUILLA associated team and by ARO under Grant No. W911NF-14-1-0011.

[1] Z. Leghtas, G. Kirchmair, B. Vlastakis, M. Devoret, R. Schoelkopf, and M. Mirrahimi, Phys. Rev. A **87**, 042315 (2013).

[2] B. Vlastakis, G. Kirchmair, Z. Leghtas, S. Nigg, L. Frunzio, S. Girvin, M. Mirrahimi, M. Devoret, and R. Schoelkopf, Science **342**, 607 (2013).

[3] M. Mirrahimi, Z. Leghtas, V. Albert, S. Touzard, R. Schoelkopf, L. Jiang, and M. Devoret, New J. Phys. **16**, 045014 (2014).

[4] V. Albert, C. Shu, S. Krastanov, C. Shen, R.-B. Liu, R. S. Z.-B. Yang, M. Mirrahimi, M. Devoret, and L. Jiang, Phys. Rev. Lett. **116**, 140502 (2016).

[5] R. Heeres, B. Vlastakis, E. Holland, S. Krastanov, V. Albert, L. Frunzio, L. Jiang, and R. Schoelkopf, Phys. Rev. Lett. **115**, 137002 (2015).

[6] C. Wang, Y. Gao, P. Reinhold, R. Heeres, N. Ofek, K. Chou, M. R. C. Axline, J. Blumoff, K. Sliwa, L. Frunzio, et al., Science **352**, 1087 (2016).

[7] L. Sun, A. Petrenko, Z. Leghtas, B. Vlastakis, G. Kirchmair, K. Sliwa, A. Narla, M. Hatridge, S. Shankar, J. Blumoff, et al., Nature **511**, 444 (2014).

[8] Z. Leghtas, G. Kirchmair, B. Vlastakis, R. Schoelkopf, M. Devoret, and M. Mirrahimi, Phys. Rev. Lett. **111**, 120501 (2013).

[9] N. Ofek, A. Petrenko, R. H. P. Reinhold, Z. Leghtas, B. Vlastakis, Y. Liu, L. Frunzio, S. Girvin, L. Jiang, M. Mirrahimi, et al., Nature **536**, 441 (2016).

[10] J. Koch, T. Yu, J. Gambetta, A. Houck, D. Schuster, J. Majer, A. Blais, M. Devoret, S. Girvin, and R. Schoelkopf, Phys. Rev. A **76**, 042319 (2007).

[11] Z. Leghtas, S. Touzard, I. Pop, A. Kou, B. Vlastakis, A. Petrenko, K. Sliwa, A. Narla, S. Shankar, M. Hatridge, et al., Science **347**, 853 (2015).

[12] M. Brune, S. Haroche, J.-M. Raimond, L. Davidovich, and N. Zagury, Physical Review A **45**, 5193 (1992).

[13] P. Facchi and S. Pascazio, Phys. Rev. Lett. **89**, 080401 (2002).

[14] V. Manucharyan and M. H. D. J. Koch, L. Glazman, Science **326**, 113 (2009).

[15] N. Masluk, I. Pop, A. Kamal, Z. Minev, and M. Devoret, Phys. Rev. Lett. **109**, 137002 (2012).

[16] I. Pop, K. Geerlings, G. Catelani, R. Schoelkopf, L. Glazman, and M. Devoret, Nature **508**, 369 (2014).

[17] V. Gramich, B. Kubala, S. Rohrer, and J. Ankerhold, Phys. Rev. Lett. **111**, 247002 (2013).

[18] M. Trif and P. Simon, Phys. Rev. B **92**, 014503 (2015).

[19] P. P. Hofer, J.-R. Souquet, and A. A. Clerk, Phys. Rev. B **93**, 041418 (2016).

[20] *See the supplementary material which includes Refs. [32]-[38].*

[21] S. Touzard, Z. Leghtas, S. Mundhada, C. Axline, K. Chou, J. Blumoff, K. Sliwa, S. Shankar, L. Frunzio, R. Schoelkopf, et al., in *APS March Meeting* (American Physical Society, 2016).

[22] A. Wallraff, D. Schuster, A. Blais, L. Frunzio, R.-Huang, J. Majer, S. Kumar, S. Girvin, and R. Schoelkopf, Nature **431**, 162 (2004).

[23] J. Gambetta, A. Blais, M. Boissonneault, A. A. Houck, D. I. Schuster, and S. M. Girvin, Phys. Rev. A **77**, 012112 (2008).

[24] J. Gambetta, A. Blais, D. I. Schuster, A. Wallraff, L. Frunzio, J. Majer, M. H. Devoret, S. M. Girvin, and R. J. Schoelkopf, Phys. Rev. A **74**, 042318 (2006).

[25] H. Paik, D. Schuster, L. Bishop, G. Kirchmair, G. Catelani, A. Sears, B. Johnson, M. Reagor, L. Frunzio, L. Glazman, et al., Phys. Rev. Lett. **107**, 240501 (2011).

[26] M. Reagor, W. Pfaff, C. Axline, R. W. Heeres, N. Ofek, K. Sliwa, E. Holland, C. Wang, J. Blumoff, K. Chou, et al., Physical Review B **94**, 014506 (2016).

[27] L. B. Ioffe, M. V. Feigel'man, A. Ioselevich, D. Ivanov, M. Troyer, and G. Blatter, Nature **415** (2002).

[28] P. Brooks, A. Kitaev, and J. Preskill, Phys. Rev. A **87** (2013).

[29] R. Azouit, A. Sarlette, and P. Rouchon, in *IEEE Conference on Decision and Control* (IEEE Conference on Decision and Control, 2015).

[30] R. Azouit, A. Sarlette, and P. Rouchon, *Adiabatic elimination for open quantum systems with effective lindblad master equations* (2016), URL `Arxiv:1603.04630`.

[31] S. Puri, S. Boutin, and A. Blais, npj Quantum Information **3**, 18 (2017).

[32] M. Mirrahimi and P. Rouchon, *Dynamics and Control of Open Quantum Systems*, Lecture notes (2015), URL `https://who.rocq.inria.fr/Mazyar.Mirrahimi/QuantSys2015.pdf`.

[33] J. Sanders and F. Verhulst, *Averaging Methods in Nonlinear Dynamical Systems* (Springer, 1987).

[34] G. Szegö, *Orthogonal polynomials*, Colloquium publications (American Mathematical Society), v. 23 (American Mathematical Society, 1939-1975), 4th ed.

[35] B. G. Korenev, *Bessel functions and their applications*, Analytical methods and special functions v.8 (Chapman & Hall/CRC, 2002), 1st ed.

[36] S. Haroche and J. Raimond, *Exploring the Quantum: Atoms, Cavities and Photons.* (Oxford University Press, 2006).

[37] A. Steane, Phys. Rev. Lett **77** (1996).

[38] M. Reagor, H. Paik, G. Catelani, L. Sun, C. Axline, E. Holland, I. Pop, N. Masluk, T. Brecht, L. Frunzio, et al., Appl. Phys. Lett. **102**, 192604 (2013).